Heliyon 10 (2024) e28310

Contents lists available at ScienceDirect

Heliyon

journal homepage: www.cell.com/heliyon

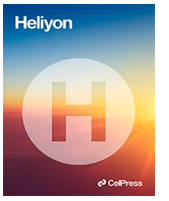

Research article

Production of bio-oil from Tung seed residues in a fluidized-bed reactor

Suntorn Suttibak *, Chayarnon Saengmanee, Athika Chuntanapum

Department of Mechanical Technology, Faculty of Technology, Udon Thani Rajabhat University, Udon Thani, 41000, Thailand

ARTICLE INFO

Keywords:
Tung seed residues
Bio-oil
Char
Fast pyrolysis
Fluidized-bed reactor

ABSTRACT

The current paper presents research on bio-oil production from Tung seed residues fed at 500 g/h *via* fast pyrolysis in a fluidized-bed. The objective was to investigate the influence of temperature on bio-oil production in a pyrolysis process. Three portions Tung residues were studied, Tung seed outer shells (TO), Tung seed inner shells (TI), and pressed residues of oil seeds (RS), all having particle sizes of 0.150–0.500 mm. The process temperatures were 350–500 °C. The physical and chemical properties of pressed residue particles were characterized by ASTM standard methods. Bio-oil component identification was done using GC-MS. Experimentally derived data showed an optimal pyrolysis temperatures for all three types of Tung residues (TO, TI and RS) of 400 °C, yielding respective maximum bio-oil yields of 53.46, 52.81, and 62.85 wt% on a dry basis (db). Apart from having highest bio-oil yield, RS produced bio-oil with the highest carbon content, leading to its greatest lower heating value (LHV), 28.05 MJ/kg (db). The main bio-oil components were acids, nitrogen compounds, and hydrocarbons. Char yield was reduced with increased temperature. Tung seed outer shells produced the highest char level (39.26 wt%) while RS gave highest char quality in term of density and heating value.

1. Introduction

Energy crops are renewable energy resources and can be classified into three main types, oil crops, sugar crops and biomass crops. They are feedstocks for producing biofuels, which can be substituted for fossil fuels [1,2]. Oil crops are the main raw materials for bio-diesel production, while sugar crops are the main feedstocks for bio-ethanol. Biomass crops can be used in various biomass energy technologies, *e.g.*, bio-gas production and combustion.

In Thailand, biodiesel is increasingly popular because it can be produced locally and used at a community level. When the transportation costs associated with biodiesel feedstocks and products are eliminated, this enables energy sustainability for a community. Among the various types of oil crops available in the country (*e.g.*, palm, Jatropha, coconut, soybean, sesame, and castor oils), Tung oil (or China wood oil) is a promising feedstock owing to its high oil. Tung seed oil is derived from Tung trees (Aleurites, Fordii or Montana). This fast-growing tree originated in China. The oil content of Tung seed is as high as 30–40 wt%, yielding a higher heating value (HHV) equal to 40.73 MJ/kg [3]. Tung oil seeds are dark brown and extremely hard. These seeds are pressed (an extraction process involving high pressure compression) to obtain oil for biodiesel production. Residues of the pressing process are the Tung seed outer shell (TO), Tung seed inner shell (TI), and residues of oil seeds that have been pressed (RS). Generally, these will be discarded, made into fertilizers, or burned as fuel.

* Corresponding author.
E-mail address: suntorn_su@hotmail.com (S. Suttibak).

https://doi.org/10.1016/j.heliyon.2024.e28310
Received 1 November 2022; Received in revised form 11 March 2024; Accepted 15 March 2024
Available online 16 March 2024

There are a number of recent research studies to improve Tung oil bio-diesel production and utilization. Novel ionic liquids can catalyze a transesterification reaction of Tung oil and methanol, resulting in higher biodiesel yields of >98% [4]. Tung oil bio-diesel, however, requires blending with other oils (*e.g.*, canola, palm, or coconut oils) or petroleum diesel to meet industrial specifications [5,6]. Performance, emissions, and combustion properties of bio-diesel blends containing Tung oil have been tested in diesel engines [7,8]. Alternatively, proper attempts to study and utilize the residues of Tung seeds are few. To date, there is a single study on the utilization of Tung seed residues using a gasification technique to obtain a producer gas [9].

Seed residues are a biomass material with high levels of oil that are amenable to pyrolysis. This is because their significant oil promotes carboxylic acid, alkane and alkene formation with other compounds as breakdown products derived from lignin, cellulose and hemicellulose decomposition. Higher bio-oil product yields are achieved with greater heating values at optimal pyrolysis temperatures ranging from 400 to 600 °C [10]. Pyrolysis may be either done by conventional or rapid processes. The former transforms biomass at a relatively low heating rate (0.1–1 K/s), at low temperatures (less than 350 °C). The process duration is long and depends on stove efficiency, biomass load and moisture content of the biomass. Three product phases (solid char, condensable vapor, and non-condensable gas) are obtained [11]. Only char is a valuable product whereas others are released into the atmosphere. Hence, conventional pyrolysis is also known as the char production process or carbonization. The other pyrolysis process transforms biomass at very high heating rates (600–1000 K/s), over a short time (1–2 s). As a consequence, the chemical structure of biomass is destroyed, changing solid biomass into various fractions, including a char and condensable vapor, along with non-condensable gases [12,13]. The primary product is condensed liquid bio-oil which is dark brown and viscous [14,15]. A maximum of 75% of the initial biomass weight (dry basis) can be converted to bio-oil. The bio-oil heating value is about half the heating value of a comparable fossil fuel [16]. In this study, fast pyrolysis is of interest since the obtained bio-oil storage and transport is not complicated. Furthermore, bio-oil can replace fuel oil for heating or electricity generation. Containing at least 200 chemicals, bio-oil is also a suitable feedstock for the chemical industry [17,18].

Research studies on fast pyrolysis have been carried out using various oil seed residues, such as groundnut shells [19], palm oil residues [20–22]. Unfortunately, fast pyrolysis for Tung seed residues has not been reported.

The current research aims to study bio-oil formation from Tung seed residues *via* fast pyrolysis. Three parts of Tung seed residues (an outer shell (TO), an inner shell (TI), and pressed residues of oil seeds (RS)) are comparatively tested. The study investigates pyrolysis temperature effects and use of various biomass portions on the product yield and physico-chemical properties of bio-oil and char products. Influence of biomass residual oil on the bio-oil product characteristics is also discussed.

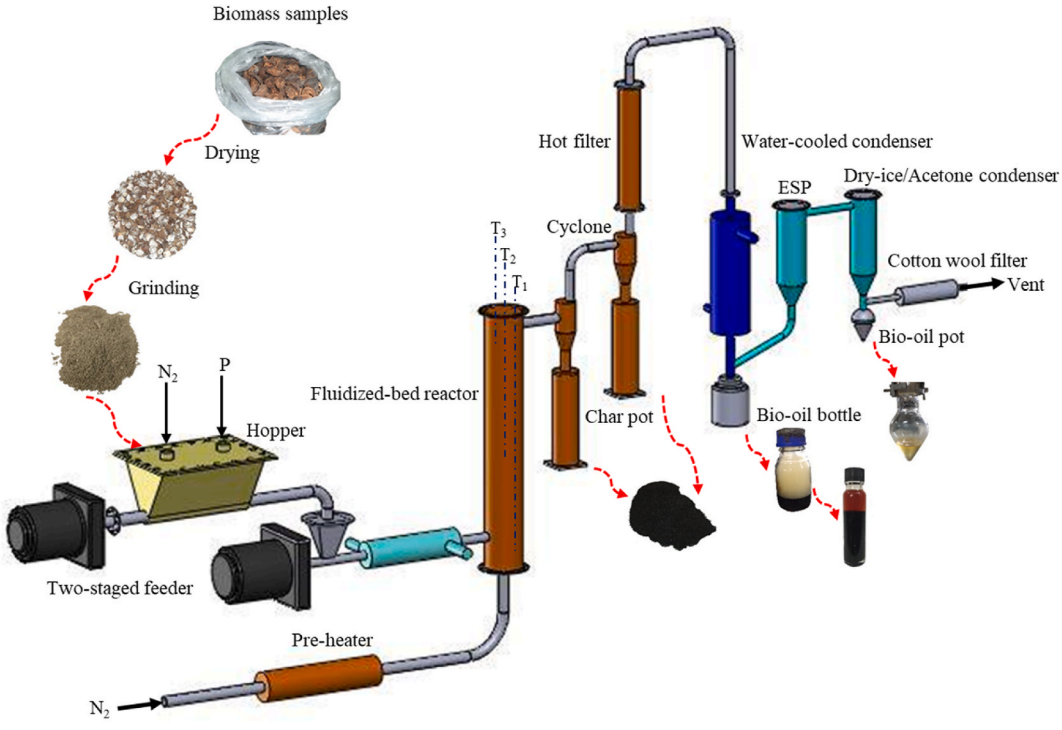

Fig. 1. Schematic drawing of experimental apparatus for the fast pyrolysis process employed the current study [23].

2. Experimental methods

2.1. Fast pyrolysis unit

Fig. 1 depicts an experimental apparatus for fast pyrolysis production of Tung seed bio-oil. The experimental setup consists of a fluidized-bed fed at 500 g/h. This apparatus consists of a hopper, a pair of screw feeders, a pre-heater, the fluidized-bed, a pair of cyclones, char pot, filter, water-cooled condenser, a 15 kV electrostatic precipitator condenser (ESP), product collection bottle, condenser cooled with dry ice/acetone, and cotton wool. The reactor was fabricated from SUS304 stainless steel, with a respective internal diameter and height of 50 and 500 mm. Silica with a particle size range of 250–500 μm was used as a medium for fluidization and heat transfer. First, biomass samples were fed to the reactor using a pair of screw feeders. Heating wires were used for the reactor and pre-heater. Ceramic fiber material insulates the reactor to mitigate heat losses. Experimental system temperature was modulated with PID temperature controllers K-type thermocouples. Vapor leaving the reactor underwent separation from char particles by the cyclone separators and a hot filtration. Hot filtration was done in a SUS304 stainless steel pipe with a 50 mm internal diameter and 300 mm height. Afterwards, the cleaned vapor was condensed to produce liquid bio-oil in a water-cooled heat exchanger, ESP, and condenser cooled by using dry ice/acetone. Finally, non-condensable gas was filtered by cotton wool before venting. Hence, no collection and analysis of the gas product was conducted.

2.2. Tung seed residue feedstock

Three parts of Tung seed residues were used, the Tung seed outer shell (TO), Tung seed inner shell (TI) and the pressed residues of oil seeds (RS), as shown in Fig. 2. To prepare for the experiments, the feedstock was dried, ground and sieved. The 0.150–0.500 mm particle size fraction was used in the experiments. It was oven dried at 105 °C for 24 h to remove H_2O before our bio-oil experiment.

Proximate analysis was done for the biomass samples to determine percent moisture, as well as volatile matter and ash, according to ASTM E1756-01, E872-82 and E1755-01 standard methods, respectively, as shown in Equations (1)–(3) [24,25]. The content of fixed carbon was determined from the residual differences (Equation (4)). Ultimate analysis (dry basis) was conducted to determine contents of carbon, hydrogen, nitrogen, sulfur, and oxygen. This was done using a Leco C, H, N, and S analyzer, Model Carbon 628 S. For comparison, heating values were obtained from both calculations and experimentation. For calculated values, the approach of Sheng and Azevedo [26], Equation (5), was employed to calculate the biomass HHV. The LHV was determined according to ECN [27], Equation (6). Both HHV and LHV are based on dry basis. For experimental values, 1 g of biomass samples was tested for heating values by bomb calorimeter, in accordance with ASTM D240 standard method. All experiments were performed in triplicate.

$$M = \frac{m_1 - m_2}{m_1} \times 100 \tag{1}$$

such that:
M = Percent moisture content (wet basis, wb),
m_1 = Initial weight of biomass (g),
m_2 = Weight of biomass after drying at 105 °C for 24 h (g).

$$V = \frac{m_2 - m_3}{m_2} \times 100 \tag{2}$$

where:
V = Volatile matter content (%, dry basis),
m_3 = Weight of biomass after burning at 970 °C for 7 min (g).

$$A = \frac{m_4}{m_2} \times 100 \tag{3}$$

where:
A = Ash content (%, dry basis),
m_4 = Weight of biomass after burning at 575 °C for 24 h (g).

$$F = 100 - V - A \tag{4}$$

where:
F = Fixed carbon content (%, dry basis).

$$HHV\left(\frac{MJ}{kg}\right) = -1.3675 + 0.3137C + 0.7009H + 0.0318O^{*} \tag{5}$$

$$LHV\left(\frac{MJ}{kg}\right) = HHV - 2.442 \times 8.936\left(\frac{H}{100}\right) \tag{6}$$

where:

Fig. 2. Three parts of Tung seed residues, Tung seed outer shell (TO), Tung seed inner shell (TI) and the pressed residues of oil seeds (RS).

C = Percent carbon content (db),
H = Percent hydrogen content (db),

O* = 100 – C – H – A.

2.3. Thermogravimetric analysis of tung seed residues

Thermogravimetric analysis (TGA) was done on Tung seed residues samples using a differential thermal analysis (DTA) with a TGA/DSC (SDT 2960 (V3.0F), TA Instruments). An N_2 gas medium was used at a heating rate of 10 °C/min. Heating the samples from room temperature to 800 °C required ~77 min.

2.4. FT-IR analysis of tung seed residues

Functional group determination of biomass feedstock was done with Fourier transform mid-infrared (FT-IR) spectroscopy. A Bruker Tensor 27 FT-IR spectrometer was used, with wavelengths of 400–4000 cm^{-1} at a 4 cm^{-1} resolution. All spectra were background-corrected. FT-IR analysis of bio-oil in the current study was not done.

2.5. Experimental conditions

Table 1 shows the experiment conditions for fast pyrolysis of Tung seed residues. Three residues, *i.e.*, Tung outer shells (TO), Tung inner shells (TI), and pressed residues of oil seeds (RS), were comparatively tested. Pyrolysis temperature was the primary parameter under focus and it was varied between 350 and 500 °C. Biomass particle sizes over the range of 0.150–0.500 mm were chosen to allow optimal fluidization and heat transfer [16]. Fine biomass particles were untimely blown out of the reactor whereas coarse particles were not heated up thoroughly. Therefore, both cases led to higher char yield. Biomass was maximally fed constant at 500 g/h and the flowrate of nitrogen gas was adjusted to 7 L/min to enable fluidization. Voltage of the electrostatic precipitator (ESP) was 15 kV to maximize bio-oil condensation [28].

2.6. Analysis of bio-oil from tung seed residues

2.6.1. Elemental composition

Bio-oil elemental composition determination was done to quantify the carbon, hydrogen, nitrogen, sulfur, and oxygen contents, using the methodology discussed in Section 2.2.

Table 1
Experimental conditions.

Parameter	Experimental conditions			
Residue type	TO, TI, RS			
Pyrolysis temperature (°C)	350	400	450	500
Biomass particle size (mm)	0.150–0.500			
Biomass feed rate (g/h)	500			
Flowrate of nitrogen gas (L/min)	7			
Heat transfer media	Sand			
ESP voltage (kV)	15			

2.6.2. Moisture content

Moister content analysis employed a Karl-Fischer Titration method. A Karl-Fisher Moisture Titrator (Model MKC-520) was also used.

2.6.3. Ash content

The content of ash was analyzed by combusting bio-oil at 775 °C for 24 h. Afterwards, the residue was considered as its ash content [29].

2.6.4. pH value

A pH meter was used to determine acidity/basicity at room temperature.

2.6.5. Density

Density of bio-oil was analyzed with a 25-mL bottle at room temperature. After filling the bottle with bio-oil, it was weighed to determine the density, according to Equation (7).

$$\rho = \frac{\mathrm{m}}{\mathrm{V}} \tag{7}$$

where: ρ = Density of bio-oil (g/mL).
m = Bio-oil mass (g).
V = Bottle volume (25 mL).

2.6.6. Heating value

Bio-oil heating values were computed from ultimate analysis data on a dry basis. The HHV was using the calculation procedures of Channiwala and Parikh [30], given as Equation (8).

$$HHV_{dry}\left(\frac{MJ}{kg}\right) = 0.3491C + 1.1783H + 0.1005S - 0.10340O - 0.0151N - 0.0211A \tag{8}$$

where C, H, O, S, N and A are the percentages of carbon, hydrogen, oxygen, sulfur, nitrogen and ash content of bio-oil on a dry basis. The LHV was calculated using the HHV and the hydrogen content, as in Equation (6). Bio-oil heating values were obtained from a bomb calorific test, similar to those of biomass, as explained in Section 2.2.

2.6.7. GC-MS

Bio-oil samples that experimentally yielded the most bio-oil (*i.e.*, at 400 °C) were analyzed by GC-MS to identify their chemical compositions. GC-MS analyzer (Agilent 7890A GC and Agilent 7000B MS) with a DB-wax capillary column (60 m length × 0.25 mm i.d., 0.25 μm film thickness). Twenty mg of the raw material was dissolved in 1 mL ethanol, and 1 μL of this material was injected into the column. The GC column was programmed to heat from 70 °C (3-min hold) at 3 °C/min to 180 °C (no time hold), and then at 10 °C/min to 250 °C (25-min hold). Injection was done in a 1:20 split mode. Helium was used as carrier gas at the flowrate of 1.0 mL/min. GC-MS data were processed by GC-QQQ software and the compounds were identified using spectral database from the NIST MS Search 2.0 library.

2.7. Analysis of char obtained from fast pyrolysis of tung seed residues

Solid char collected from the cyclones in experiments with the greatest bio-oil yields (*i.e.*, 400 °C) was used for characterization. Elemental composition of these samples was determined, as were the density, ash content, and heating values. Each analysis was performed in triplicate.

2.7.1. Elemental composition

Char elemental composition was quantified yielding carbon, hydrogen, nitrogen, sulfur, and oxygen levels. This was done in an identical manner as for the biomass feedstock and bio-oil, discussed in Section 2.2.

2.7.2. Density

Char density was analyzed using a 50-mL bottle at room temperature. After filling the bottle with char particles, it was weighed to determine the density, according to Equation (7).

2.7.3. Ash content

Ash content determination is discussed in Section 2.2.

2.7.4. Heating values

Heating values of char were calculated determined using Equations (6) and (8) for LHV and HHV, respectively.

3. Results and discussion

3.1. Biomass characterization

Table 2 presents the properties of three types of Tung seed residues. The proximate analysis results show RS with the highest volatile matter content, 79.46 wt% (dry basis). Thus, it can be speculated that RS will have higher bio-oil yields than TI and TO fractions. From an ultimate analysis, RS has a higher carbon content (50.30 wt% on a dry basis) than TO and TI. Comparing with earlier research studies, RS presents a higher carbon content than groundnut shells [19] but less than palm shells [31]. In fact, the carbon content greatly contributes to the biomass heating value. A greater carbon content yields an augmented heating value. As a result, RS has a higher LHV (19.00 MJ/kg) than TO and TI. Despite being approximately 5% higher than those of calculated ones, experimented heating value (HHV) by bomb calorimeter showed the same tendency, with RS having the highest value at 21.15 MJ/kg.

Fig. 3 presents thermogravimetric analysis (TGA) of TO, TI and RS. As can be seen from this graph, the first mass loss of Tung seed residue occurred at about 25–100 °C. This resulted from water loss from the biomass. The next mass loss was observed at temperatures of 220–350 °C for TO and TI, and 220–400 °C for RS, resulting from hemicellulose and cellulose decomposition. Lignin was the last component to decompose, at 450–1000 °C, as can be seen by the tail of the graph for the three types of Tung seed residues in Fig. 3. The weight loss characteristics of Tung seed residues were similar to those of bagasse [23], radiata pine [32], biomass pellets [33], and straw [34,35] over all temperature ranges examined.

Biomass compositional structure and functional group were characterized by FT-IR technique. FT-IR spectra of TO and TI showed similarities while that of RS has distinctive pattern and intensity, particularly within a wavelength of 1700–1000 cm^{-1} (Fig. 4). For RS graph, shaper peaks attributed to C–C, C–O bonds (1230 cm^{-1}), and aromatic rings (1269 and 1502 cm^{-1}) [36] were noticed. This implied a presence of lignin component in RS. Furthermore, RS graph had boarder peak at 1622 cm^{-1}, corresponding to C=O bonds in hemicellulose and triglycerides [10]. All type of biomass showed the same peaks at 1026 (C–O), 1142 (C–O–C), and 1734 (C=O) cm^{-1} [36], indicating cellulose and hemicellulose composition.

3.2. Effect of pyrolysis temperature on bio-oil production

Fig. 5 shows the impacts of pyrolysis temperature on bio-oil yield. The results clearly showed an optimal pyrolysis temperature for all types of Tung seed residues at 400 °C. The greatest bio-oil yields achieved were 53.46, 52.81 and 62.85 wt%, for TO, TI, and RS, respectively. All parts of Tung seed residues produced more bio-oil than palm residues, which was 46.4 wt% [31]. However, it is notable that performance differences might be partially due to the disparate reactors used in palm residue experiments.

From Fig. 6, two phases can be clearly seen in bio-oils, oil and aqueous phases. An oil phase can be used as bio-fuel whereas water phase is a potential feedstock for the bio-chemical industry. Bio-oils obtained from TO and TI have the same phase characteristics, with the organic phase being denser. In contrast, RS bio-oil obtained produced an organic phase that was less dense than an aqueous phase.

Fig. 7 shows the relative amounts of two phases of bio-oil obtained from three types of Tung seed residues pyrolyzed at 400 °C (optimal temperature). Not only does the bio-oil from RS have unique phase characteristics, but also the amount of oil phase was six-times greater than that of the aqueous phase. This is because the RS still had some residual oil after pressing, and the experimental

Table 2
Characteristics of Tung seed residues.

Analysis	Tung seed residues			Groundnut shells[a]	Palm shells[b]
	TO	TI	RS		
Proximate analysis (wt.%, dry basis)					
Moisture (wet basis)	0.25 ± 0.13	5.55 ± 0.07	0.23 ± 0.01	4.01	11.00
Volatile matter	66.81 ± 0.16	65.07 ± 0.21	79.46 ± 0.51	70.46	74.59
Fixed carbon*	22.96 ± 0.15	26.27 ± 0.06	12.93 ± 0.45	12.16	21.87
Ash	10.23 ± 0.01	8.36 ± 0.16	7.60 ± 0.07	17.22	2.33
Ultimate analysis (wt.%, dry basis)					
Carbon	43.00 ± 0.08	49.73 ± 0.14	50.30 ± 0.07	36.62	55.89
Hydrogen	5.96 ± 0.02	6.64 ± 0.04	7.21 ± 0.12	5.73	5.98
Nitrogen	0.56 ± 0.02	1.92 ± 0.08	4.70 ± 0.09	3.11	0.09
Sulfur	0.06 ± 0.01	0.18 ± 0.02	0.34 ± 0.04	0.23	0.18
Oxygen*	40.19	33.15	29.85	37.06	35.51
H/C molar ratio	1.66 ± 0.01	1.60 ± 0.01	1.30 ± 0.05	1.88	1.28
O/C molar ratio	0.70 ± 0.01	0.50 ± 0.01	0.24 ± 0.02	0.76	0.48
Molecular formula	$CCH_{1.66}O_{0.70}$	$CH_{1.60}O_{0.50}$	$CH_{1.30}O_{0.24}$	$CH_{1.88}O_{0.76}$	$CH_{1.28}O_{0.48}$
Heating value by calculation (MJ/kg, dry basis)					
Higher heating value (HHV)	17.60 ± 0.02	20.01 ± 0.05	20.57 ± 0.10	15.42	21.47
Lower heating value (LHV)	16.30 ± 0.02	18.56 ± 0.05	19.00 ± 0.07	14.17	20.16
Heating value by bomb calorimeter (MJ/kg)					
Higher heating value (HHV)	19.52 ± 0.22	20.50 ± 0.10	21.15 ± 0.06	n/a	n/a

* Calculated by difference.
[a] Suttibak [19].
[b] Abnisa et al. [31].

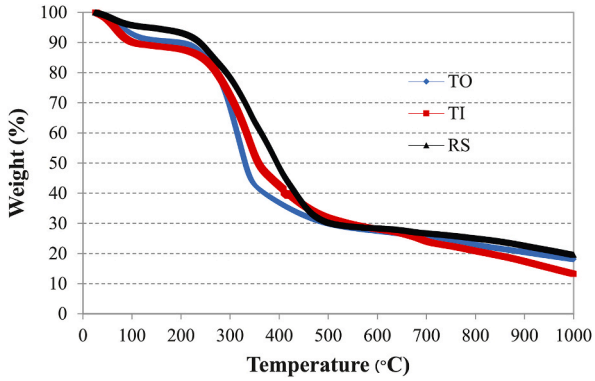

Fig. 3. Thermogravimetric analysis of Tung seed residues, Tung seed outer shell (TO), Tung seed inner shell (TI) and the pressed residues of oil seeds (RS).

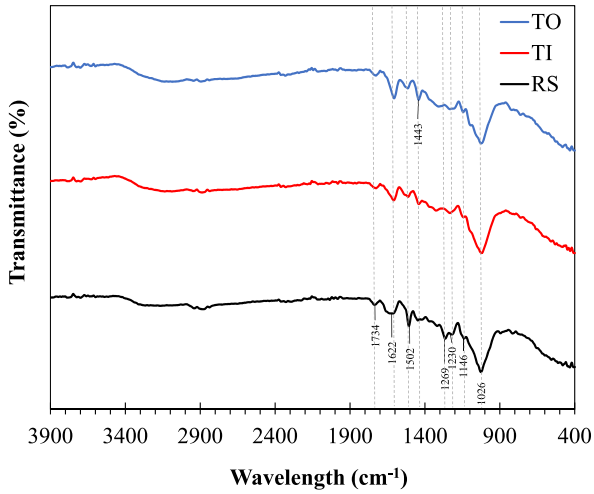

Fig. 4. FT-IR spectra of Tung seed residues, Tung seed outer shell (TO), Tung seed inner shell (TI) and the pressed residues of oil seeds (RS).

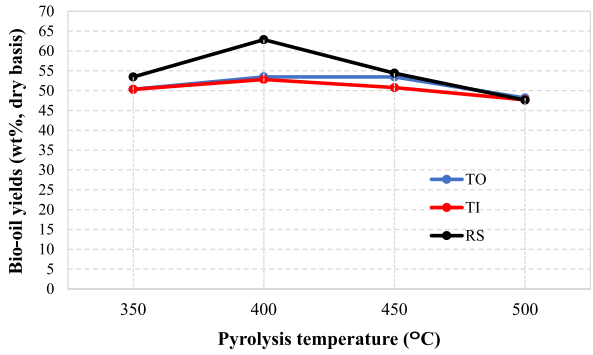

Fig. 5. Effect of temperature on bio-oil yield from different parts of Tung seed residues, Tung seed outer shell (TO), Tung seed inner shell (TI) and the pressed residues of oil seeds (RS).

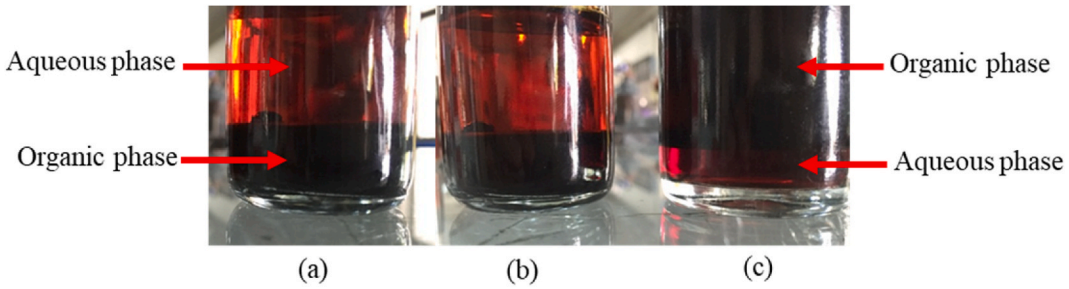

Fig. 6. Phase separation/arrangement characteristic of bio-oil obtained from three types of Tung seed residues, (a) TO, (b) TI, (c) RS.

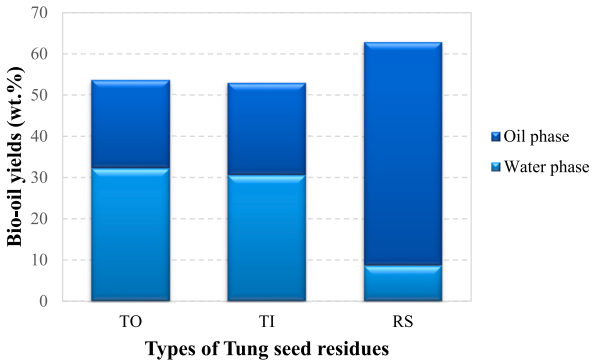

Fig. 7. Comparison of bio-oil yields in oil and water phases at 400 °C (optimal temperature).

Table 3
The properties of bio-oils obtained from Tung seed residues.

Types of oil/bio-oil	Analysis parameters			
	Water content (wt.%)	Density (kg/m^3)	pH value	Ash content (wt.%)
Tung oil	0.25 ± 0.15	920.1 ± 7.60	5.22 ± 0.11	NA
TO-Bio oil (Aqueous phase)	89.45 ± 16.42	990.1 ± 1.01	4.69 ± 0.02	NA
TO-Bio oil (Organic phase)	18.73 ± 0.26	1139.5 ± 62.32	4.60 ± 0.03	0.03 ± 0.01
TI-Bio oil (Aqueous phase)	85.12 ± 22.58	998.3 ± 0.99	4.09 ± 0.02	NA
TI-Bio oil (Organic phase)	14.68 ± 0.68	1147.2 ± 29.40	3.74 ± 0.12	0.02 ± 0.01
RS-Bio oil (Aqueous phase)	86.88 ± 21.36	1026.3 ± 3.57	6.60 ± 0.01	NA
RS-Bio oil (Organic phase)	8.06 ± 0.43	966.4 ± 0.46	8.09 ± 0.09	0.01 ± 0.01
Bio-oil from groundnut shells[a]	18.56	1215	4.2	0.03
Bio-oil obtained from palm residue[b]	53	1051	2.5	NA
Bio-oil obtained from Napier grass[c] (Aqueous phase)	73.32 ± 19.3	993 ± 2.21	4.42 ± 0.02	<0.01 ± 0.003
Bio-oil obtained from Napier grass[c] (Organic phase)	9.40 ± 0.65	1101 ± 2.07	4.22 ± 0.02	0.01 ± 0.004
ASTM burner fuel standards[d]	30 max	1,100–1,300	2 - 4	0.25 max

[a] Suttibak [19].
[b] Abnisa et al. [31].
[c] Junsiri and Suttibak [32].
[d] Oasmaa et al. [33].

results show that fast pyrolysis can help extract this oil content.

3.3. Characterization of bio-oil products

Table 3 compares the bio-oils derived from three Tung seed residues *via* fast pyrolysis. Characterization was conducted for both organic and aqueous phases, however, only the organic phase can serve as a bio-fuel. Therefore, it is the only phase considered in the current work. The bio oils from TO, TI, and RS had water contents of 18.73, 14.68, and 8.06 wt%, respectively. The moisture content of the RS bio-oil organic phase was lowest, while those of TO and TI had the same magnitude as that of bio-oil produced from groundnut shells [19]. All types of Tung seed residues could produce bio-oil with much less water content than that of palm residues [31]. The densities of bio-oil from TO, TI and RS were 1139.5, 1147.2 and 966.4 kg/m^3, respectively. It is notable that the bio-oil from RS was less dense than water. In contrast, the bio-oil from TO and TI was denser than water, which is similar to that of Napier grass bio-oil

Table 4
Analysis of element composition and heating values of bio-oils.

Analysis	Bio-oil from Tung seed residues (Organic phase)			Tung oil	Groundnuts shell[a]	Palm shells[b]
	TO	TI	RS			
Pyrolysis temperature (°C)	400	400	400		475	500
Elemental composition (wt.%, dry basis)						
Carbon	60.63 ± 0.53	64.22 ± 0.36	66.85 ± 1.39	77.75 ± 0.56	71.46	19.48
Hydrogen	4.56 ± 0.03	5.67 ± 0.03	7.25 ± 0.13	8.97 ± 0.13	7.73	8.92
Nitrogen	0.43 ± 0.06	1.84 ± 0.09	4.32 ± 0.11	4.44 ± 0.12	6.57	0.2
Sulfur	0.06 ± 0.02	0.13 ± 0.01	0.21 ± 0.02	1.24 ± 0.07	1.35	0.04
Oxygen*	34.52	28.10	21.35	7.59	12.86	71.40
H/C molar ratio	0.91 ± 0.01	1.06 ± 0.01	1.30 ± 0.05	1.39 ± 0.01	1.30	NA
O/C molar ratio	0.43 ± 0.01	0.33 ± 0.01	0.24 ± 0.02	0.07 ± 0.01	0.13	NA
Molecular formula	$CH_{0.91}O_{0.43}$	$CCH_{1.06}O_{0.33}$	$CH_{1.30}O_{0.24}$	$CH_{1.39}O_{0.07}$	$CH_{1.30}O_{0.13}$	NA
Heating value by calculation method (MJ/kg, dry basis)						
Higher Heating Value (HHV)	22.89 ± 0.22	26.19 ± 0.14	29.63 ± 0.47	36.99 ± 0.41	26.68	11.94
Lower Heating Value (LHV)	21.89 ± 0.22	24.95 ± 0.14	28.05 ± 0.47	35.03 ± 0.38	24.85	10.0
Heating value by bomb calorimeter (MJ/kg)						
Higher heating value (HHV)	21.32 ± 0.03	24.69 ± 0.02	28.11 ± 0.05	35.79 ± 0.07	n/a	n/a

* Calculated using a difference.
[a] Suttibak [19].
[b] Abnisa et al. [31].

[37]. Tung oil has a density of approximately 920 kg/m^3. It was expected that Tung oil left in the RS was extracted into the organic phase, and this gave rise to the lower density for RS bio-oil among the other Tung seed residues. The bio-oil pH values were 4.60, 3.74, and 8.09, for TO, TI, and RS respectively. Except for the caustic nature of RS bio-oil, other bio-oil properties were close to the ASTM burner fuel standards [38] for all samples.

Table 4 presents the ultimate analysis and heating values of bio-oil obtained from fast pyrolysis of three Tung seed residues. Among all types of Tung seed residues, the RS bio-oil showed the most carbon, leading to its highest heating value. This was primarily caused by residual Tung oil in RS after pressing. Tung oil has a carbon content as high as 77.75 wt% (dry basis) and this gave rise to the greater carbon content in RS bio-oil. Carbon is the main source of heat in biomass. Greater carbon contents indicate higher heating values. Comparing to bio-oil from groundnut shells [19], TI and RS yielded bio-oil with higher heating values, while TO derived bio-oil had a lower heating value. Bio-oil from all three types of Tung seed residues had significantly higher heating values than that of bio-oil of palm shells [31]. Experimental bio-oil HHV values were roughly 6% lower than the calculated HHV for all three samples. Apparently, the same increasing trend of heating values from TO, TI to RS could be observed.

Experimentally obtained bio-oil chemical composition (organic phase) with the highest bio-oil yield (*i.e.*, 400 °C) for three types of feedstocks was identified using a GC-MS technique. Semi-quantitative analysis was done based on percent of peak area of 6 chemical groups. It was computed from sum of peak area of each chemical group divided by total peak area. As shown in Fig. 8 in descending order of intensities, they are acids, nitrogen compounds, hydrocarbons, phenols, ketones, and esters [10]. List of individual chemicals was provided in Supplementary material 1.

The GC-MS analysis revealed similar chemical composition and proportion among 3 different kinds of Tung seed residues (Fig. 8). Acids were the most abundant chemicals in bio-oil, with 62.6–64.7% of quantified area. Nitrogen compounds and hydrocarbons were ranked second and third, with 14.8–15.5% and 12.0–13.5% of quantified area, respectively. For oil-containing biomass, acids and hydrocarbons were the main decomposition products. This is because triglycerides were pyrolyzed into carboxylic acids, fatty acids, alkenes, alkanes, alkadienes, and aromatic hydrocarbons [10]. For nitrogen compounds, Tung seed residues tended to result in more nitrogen compounds in bio-oil than other biomasses in earlier works. Bio-oil from mangaba seed [10] yielded nitrogen compounds in comparable amount to phenols, ketones, esters and alcohols. Bio-oil from sugarcane bagasse [39], hardwood sawdust [40] and palm kernel shell [41] showed no presence in nitrogen compounds. While the optimum pyrolytic temperature of other biomasses in the literature was in the range of 500–650 °C [10,39–43], the present study showed 400 °C was the best condition for bio-oil production. Therefore, lower pyrolytic temperature was expected to cause less gasification of protein content in Tung seed residues, leading to more nitrogen compounds remained in bio-oil. Phenols and ketones had their quantified area in the same order of magnitude. Whereas phenols were mainly derived from lignin, ketones were originated from cellulose and hemicellulose [10,39,41].

As shown in Fig. 9, the number of C atoms in acids was plotted against the peak area of GC-MS chromatogram [10]. The peak area of C16 and C18 appeared distinguishably high. The remaining of large acid molecules in bio-oil dictated partial decomposition of oil content in Tung seed residues. C16 acids consisted of palmitic acid, and C18 acids were composed of stearic acid, oleic acid, and linoleic acid. Besides these large fatty acids, the majority of carbon chain of acidic components in bio-oil was C5 – C10.

3.4. Pyrolysis temperature impacts on char yield

Temperature effects on char yield were different from those of bio-oil. While a peak was observed at 400 °C for bio-oil (Fig. 5), char yield kept decreasing with increasing temperature (Fig. 10). At higher temperatures, not only was there more primary biomass decomposition, but secondary thermal decomposition of solid char took place as well [16]. Among three sample types, TO gave the

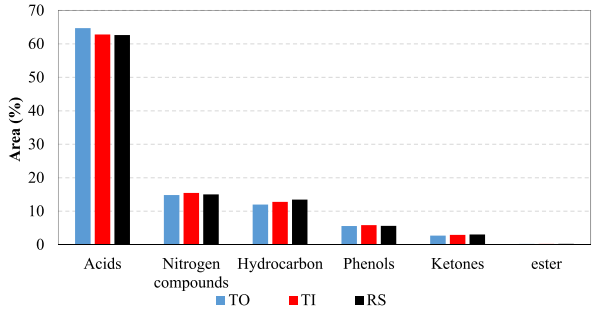

Fig. 8. Distribution of chemical groups in bio-oil obtained from the experiment at 400 °C (optimal temperature) from different parts of Tung seed residues, Tung seed outer shell (TO), Tung seed inner shell (TI) and the pressed residues of oil seeds (RS).

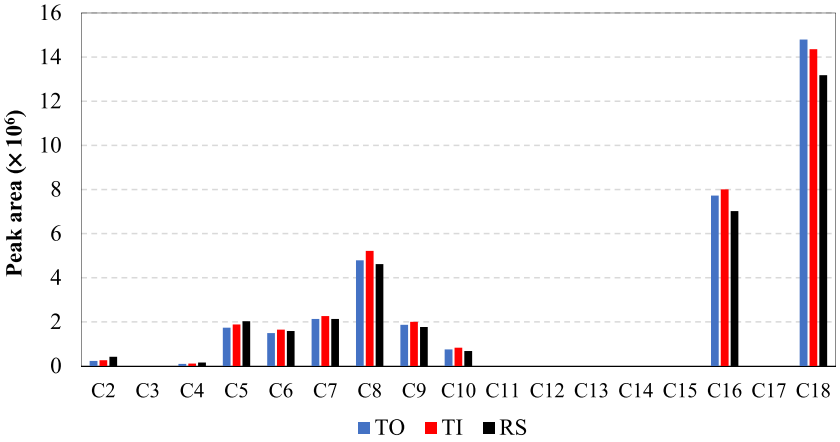

Fig. 9. Carbon number distribution of acid compounds in bio-oil obtained from the experiment at 400 °C (optimal temperature) from different parts of Tung seed residues, Tung seed outer shell (TO), Tung seed inner shell (TI) and the pressed residues of oil seeds (RS).

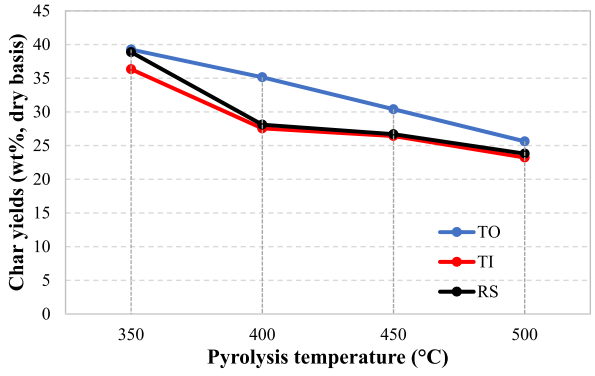

Fig. 10. Effect of temperature on char yield from different parts of Tung seed residues, Tung seed outer shell (TO), Tung seed inner shell (TI) and the pressed residues of oil seeds (RS).

highest yield of char particles at all temperatures, whereas TI and RS produced similar level of the yield.

3.5. Characterization of char products

Table 5 presents char characteristics from fast pyrolysis of TO, TI, and RS. Char from RS showed outstanding properties. It had the highest carbon content and density, resulting in its highest heating values. Hence, this indicated that residual oil was also beneficial in the quality of solid char. Ultimate analysis indicates that the H/C molar ratios were 0.53–0.56 with O/C molar ratios of 0.03–0.05 for all three cases.

Table 5
Characteristics of char product from fast pyrolysis of Tung seed residues.

Analysis	Char from Tung seed residues			Groundnuts shell[a]
	TO	TI	RS	
Pyrolysis temperature (°C)	400	400	400	475
Elemental composition (wt.%, dry basis)				
Carbon	65.27 ± 0.50	67.28 ± 0.85	72.23 ± 0.91	61.78
Hydrogen	2.87 ± 0.05	3.07 ± 0.05	3.37 ± 0.09	3.56
Nitrogen	1.04 ± 0.07	1.15 ± 0.03	1.36 ± 0.09	2.75
Sulfur	0.67 ± 0.09	0.87 ± 0.11	0.81 ± 0.06	0.60
Oxygen*	4.43	3.77	2.89	0.64
H/C molar ratio	0.53 ± 0.01	0.55 ± 0.01	0.56 ± 0.01	0.69
O/C molar ratio	0.05 ± 0.01	0.04 ± 0.01	0.03 ± 0.01	0.11
Molecular formula	$CH_{0.53}O_{0.05}$	$CH_{0.55}O_{0.04}$	$CH_{0.56}O_{0.03}$	$CH_{0.69}O_{0.11}$
Density (kg/m^3)	208.04 ± 0.44	286.77 ± 1.62	494.98 ± 0.68	NA
Ash (wt.%)	26.39 ± 0.63	24.73 ± 0.72	20.15 ± 0.30	22.98
Heating value by calculation method (MJ/kg, dry basis)				
HHV	25.14 ± 0.24	26.18 ± 0.44	28.44 ± 0.49	24.34
LHV	24.52 ± 0.23	25.51 ± 0.43	27.71 ± 0.47	23.56

* Calculated using a difference.
[a] Suttibak [19].

4. Conclusions

Product characterization from fast pyrolysis process of Tung seed residues in a fluidized-bed reactor was done, with a 500 g/h feed rate. An optimal pyrolysis temperature for TO, TI and RS was 400 °C, respectively producing 53.46, 52.8 and 62.85 wt% of bio-oil yield (dry basis). Among three types of Tung seed residues, maximal bio-oil yield was from RS. The bio-oils clearly separated, forming organic and aqueous phases. Organic phases of these three bio-oils had moisture contents of 18.73, 14.68, and 8.06 wt%, with densities of 1139.5, 1147.2, and 966.4 kg/m^3, for TO, TI and RS, respectively. The organic phase of bio-oil obtained from RS had a density less than water. Furthermore, bio-oil from RS had the highest percentage of carbon and subsequently the highest heating value. From GC-MS result, bio-oil chemical composition was found to be dominant by acids, nitrogen compounds, and hydrocarbons. This occurred since there was still residual Tung oil in the seed residue after oil pressing. Therefore, a conclusion is drawn that pyrolysis is an alternative approach to maximize use of oil-rich Tung seed residues. Residual oil in Tung seeds has an important part in both the quality and quantity of bio-oil product obtained. Bio-oil had the properties that were close to the ASTM burner-fuel standards and therefore could be used as a bio-fuel. Char product showed lower yield with increasing temperature, owing to its subsequent thermal degradation. TO gave the highest char yield, 39.26 wt% at 350 °C. In contrast, TI produced minimal char yield, 23.23 wt% at 500 °C. At 400 °C, RS generated char with the highest density of 494.98 kg/m^3 and LHV of 27.71 MJ/kg. Hence, residual oil in Tung seeds also impacted the quality of char product obtained.

Data availability statement

Data will be made available on request.

CRediT authorship contribution statement

Suntorn Suttibak: Writing – original draft, Supervision, Methodology, Investigation, Funding acquisition, Formal analysis, Data curation, Conceptualization. **Chayarnon Saengmanee:** Resources, Project administration, Methodology, Investigation. **Athika Chuntanapum:** Writing – review & editing, Writing – original draft, Visualization, Validation, Resources, Formal analysis.

Declaration of competing interest

The authors declare that they have no known competing financial interests or personal relationships that could have appeared to influence the work reported in this paper.

Acknowledgements

Financial support from the Energy Policy and Planning Office (EPPO 060/2558), Ministry of Energy, Thailand, Royal Thai Government, is gratefully acknowledged. We also appreciate the efforts of Prof. Jeffrey Nash, Mr. Kamolwit Arsasoi, Mr. Teerawat Kanhala and Mr. Adisak Kamta for their research assistance. The authors thank Udon Thani Rajabhat University for supporting this research.

Appendix A. Supplementary data

Supplementary data to this article can be found online at https://doi.org/10.1016/j.heliyon.2024.e28310.

References

[1] K. Akubo, M.A. Nahil, P.T. Williams, Pyrolysis-catalytic steam reforming of agricultural biomass wastes and biomass components for production of hydrogen/syngas, J. Energy Inst. 92 (2019) 1987–1996, https://doi.org/10.1016/j.joei.2018.10.013.

[2] V. Tilvikienea, Z. Kadziuliene, I. Liaudanskiene, E. Zvicevicius, Z. Cerniauskiene, A. Cipliene, A.J. Raila, J. Baltrusaitis, The quality and energy potential of introduced energy crops in northern part of temperate climate zone, Renew. Energy 151 (2020) 887–895, https://doi.org/10.1016/j.renene.2019.11.080.

[3] L. Zhang, M. Liu, H. Long, W. Dong, A. Pasha, E. Esteban, W. Li, et al., Tung tree (Vernicia fordii) genome provides a resource for understanding genome evolution and improved oil production, Dev. Reprod. Biol. 17 (2019) 558–575, https://doi.org/10.1016/j.gpb.2019.03.006.

[4] J. Yang, Y. Feng, T. Zeng, X. Guo, L. Li, R. Hong, T. Qiu, Synthesis of biodiesel via transesterification of tung oil catalyzed by new Brönsted acidic ionic liquid, Chem. Eng. Res. Des. 117 (2017) 584–592, https://doi.org/10.1016/j.cherd.2016.09.038.

[5] Y.H. Chen, J.H. Chen, C.Y. Chang, C.C. Chang, Biodiesel production from tung (Vernicia Montana) oil and its blending properties in different fatty acid compositions, Bioresour. Technol. 101 (24) (2010) 9521–9526, https://doi.org/10.1016/j.biortech.2010.06.117.

[6] Y.H. Chen, J.H. Chen, Y.M. Luo, Complementary biodiesel combination from tung and medium-chain fatty acid oils, Renew. Energy 44 (2012) 305–310, https://doi.org/10.1016/j.renene.2012.01.098.

[7] P.S. Ranjit, S.K. Basha, S.S. Bhurat, A. Thakur, A.V. Babu, G.S. Mahesh, M.S. Reddy, Enhancement of performance and reduction in emissions of hydrogen supplemented Aleurites fordii biodiesel blend operated diesel engine, Int. J. Veh. Struct. Syst. 14 (2) (2022) 174–178, https://doi.org/10.4273/ijvss.14.2.08.

[8] H. Harish, S. Rajanna, G.S. Prakash, S. Muzzamil Ahamed, Extraction of biodiesel from tung seed oil and evaluating the performance and emission studies on 4-stroke CI engine, Mater, Today Proc. 46 (2021) 4869–4877, https://doi.org/10.1016/j.matpr.2020.10.328.

[9] L. Prasad, B.L. Salvi, V. Kumar, Thermal degradation and gasification characteristics of Tung Shells as an open top downdraft wood gasifier feedstock, Clean Technol. Environ. Policy 17 (2015) 1699–1706, https://doi.org/10.1007/s10098-014-0891-8.

[10] R.M. Santos, A.O. Santos, E.M. Sussuchi, J.S. Nascimento, Á.S. Lima, L.S. Freitas, Pyrolysis of mangaba seed: production and characterization of bio-oil, Bioresour. Technol. 196 (2015) 43–48, https://doi.org/10.1016/j.biortech.2015.07.060.

[11] A.V. Bridgwater, Review of fast pyrolysis of biomass and product upgrading, Biomass Bioenergy 38 (2012) 68–94, https://doi.org/10.1016/j.biombioe.2011.01.048.

[12] P.F. Prashanth, M.M. Kumar, R. Vinu, Analytical and microwave pyrolysis of empty oil palm fruit bunch: kinetics and product characterization, Bioresour. Technol. 310 (2020) 123394, https://doi.org/10.1016/j.biortech.2020.123394.

[13] C. Zhang, Z. Zhang, L. Zhang, Q. Li, C. Li, G. Chen, S. Zhang, Q. Liu, X. Hu, Evolution of the functionalities and structures of biochar in pyrolysis of poplar in a wide temperature range, Bioresour. Technol. 304 (2020) 123002, https://doi.org/10.1016/j.biortech.2020.123002.

[14] K. Duanguppama, N. Suwapaet, A. Pattiya, Fast pyrolysis of contaminated sawdust in a circulating fluidised bed reactor, J. Anal. Appl. Pyrolysis 118 (2016) 63–74, https://doi.org/10.1016/j.jaap.2015.12.025.

[15] S. Suttibak, K. Sriprateep, A. Pattiya, Production of bio-oil from pine sawdust by rapid pyrolysis in a fluidised-bed reactor, energy sources Part A recovery util, Environ. Eff. 37 (2015) 1440–1446, https://doi.org/10.1080/15567036.2011.631091.

[16] A. Pattiya, S. Suttibak, Production of bio-oil via fast pyrolysis of agricultural residues from cassava plantations in a fluidised-bed reactor with a hot vapour filtration unit, J. Anal. Appl. Pyrolysis 95 (2012) 227–235, https://doi.org/10.1016/j.jaap.2012.02.010.

[17] B. Fekhar, L. Gombor, N. Miskolczi, Pyrolysis of chlorine contaminated municipal plastic waste: in-situ upgrading of pyrolysis oils by Ni/ZSM-5, Ni/SAPO-11, red mud and $Ca(OH)_2$ containing catalysts, J. Energy Inst. 92 (2019) 1270–1283, https://doi.org/10.1016/j.joei.2018.10.007.

[18] Q. Lu, W.Z. Li, X.F. Zhu, Overview of fuel properties of biomass fast pyrolysis oils, Energy Convers. Manag. 50 (2009) 1376–1383, https://doi.org/10.1016/j.enconman.2009.01.001.

[19] S. Suttibak, Characterization of bio-oil produced obtained from fast pyrolysis of groundnuts shell, Int. J. Biosci. 3 (2013) 82–89, https://doi.org/10.1016/j.biombioe.2013.08.037.

[20] S.W. Kim, B.S. Koo, D.H. Lee, Catalytic pyrolysis of palm kernel shell waste in fluidized bed, Bioresour. Technol. 167 (2014) 425–432, https://doi.org/10.1016/j.biortech.2014.06.050.

[21] M. Asadullah, N.S.A. Rasid, S.A.S.A. Kadir, A. Azdarpour, Production and detailed characterization of bio-oil from fast pyrolysis of palm kernel shell, Biomass Bioenergy 59 (2013) 316–324, https://doi.org/10.1016/j.biombioe.2013.08.037.

[22] F. Abnisa, W.M.A. Wan Daud, W.N.W. Husin, J.N. Sahu, Utilization possibilities of palm shell as a source of biomass energy in Malaysia by producing bio-oil in pyrolysis process, Biomass Bioenergy 35 (2011) 1863–1872, https://doi.org/10.1016/j.biombioe.2011.01.033.

[23] S. Suttibak, Influence of reaction temperature on yields of bio-oil from fast pyrolysis of sugarcane residues, Eng. Appl. Sci. Res. 44 (2017) 142–147, https://doi.org/10.14456/easr.2017.21.

[24] A. Pattiya, S. Suttibak, Fast pyrolysis of sugarcane residues in a fluidised bed reactor with a hot vapour filter, J. Energy Inst. 90 (2017) 110–119, https://doi.org/10.1016/j.joei.2015.10.001.

[25] A. Pattiya, Thermochemical characterization of agricultural wastes from Thai cassava plantations, Energy Sources Part A Recovery Util, Environ. Eff. 33 (2011) 691–701, https://doi.org/10.1080/15567030903228922.

[26] C.D. Sheng, J.L.T. Azevedo, Estimating the higher heating value of biomass fuels from basic analysis data, Biomass Bioenergy 28 (2005) 499–507, https://doi.org/10.1016/j.biombioe.2004.11.008.

[27] Phyllis Ecn, Database for Biomass and Waste, Energy Research Centre of the Netherlands (ECN), 2017, https://doi.org/10.1080/15567036.2021.1941438. http://www.ecn.nl/phyllis/defs.asp. (Accessed 1 April 2017).

[28] S. Suttibak, N. Kokasath, C. Uampawa, Effect of electrostatic precipitator condenser voltage on bio-oil yields obtained from fast pyrolysis of water hyacinth, Udon Thani Rajabhat University Journal of Sciences and Technology 3 (2015) 41–51, https://doi.org/10.1627/jpi.56.401.

[29] A.P. Oasmaa, C. Peacocke, Properties and fuel use of biomass derived fast pyrolysis liquids: a guide, VTT Publ. 731 (2010) 1–134, https://doi.org/10.13140/RG.2.2.32703.20649.

[30] S.A. Channiwala, P.P. Parikh, A unified correlation for estimating HHV of solid, liquid and gaseous fuels, Fuel 81 (2002) 1051–1063, https://doi.org/10.1016/S0016-2361(01)00131-4.

[31] F. Abnisa, W.M.A. Wan Daud, J.N. Sahu, Optimization and characterization studies on bio-oil production from palm shell by pyrolysis using response surface methodology, Biomass Bioenergy 35 (2011) 3604–3616, https://doi.org/10.1016/j.biombioe.2011.05.011.

[32] B.S. Kang, K.H. Lee, H.J. Park, Y.K. Park, J.S. Kim, Fast pyrolysis of radiata pine in a bench scale plant with a fluidized bed: influence of a char separation system and reaction conditions on the production of bio-oil, J. Anal. Appl. Pyrolysis 76 (2006) 32–37, https://doi.org/10.1016/j.jaap.2005.06.012.

[33] F. Guo, Y. He, A. Hassanpour, J. Gardy, Z. Zhong, Thermogravimetric analysis on the co-combustion of biomass pellets with lignite and bituminous coal, Energy 197 (2020) 117147, https://doi.org/10.1016/j.energy.2020.117147.

[34] F. Sher, S.Z. Iqbal, H. Liu, M. Imran, C.E. Snape, Thermal and kinetic analysis of diverse biomass fuels under different reaction environment: a way forward to renewable energy sources, Energy Convers. Manag. 203 (2020) 112266, https://doi.org/10.1016/j.enconman.2019.112266.

[35] S.H. Jung, B.S. Kang, J.S. Kim, Production of bio-oil from rice straw and bamboo sawdust under various reaction conditions in a fast pyrolysis plant equipped with a fluidized bed and a char separation system, J. Anal. Appl. Pyrolysis 82 (2008) 240–247, https://doi.org/10.1016/j.jaap.2008.04.001.
[36] F. Xu, J. Yu, T. Tesso, F. Dowell, D. Wang, Qualitative and quantitative analysis of lignocellulosic biomass using infrared techniques: a mini-review, Appl. Energy 104 (2013) 801–809, https://doi.org/10.1016/j.apenergy.2012.12.019.
[37] R. Junsiri, S. Suttibak, Effect of reaction temperatures on yields and properties of bio-oil produced by fast pyrolysis of Napier Pak Chong 1 grass (Pennisetum Purpureum Schum), J. Mater. Sci. Appl. Energy 5 (2016) 18–21, https://doi.org/10.1016/j.fuel.2012.12.018.
[38] A. Oasmaa, D.C. Elliott, S. Muller, Quality control in fast pyrolysis bio-oil production and use, Energy Convers. Manag. 28 (2009) 404–409, https://doi.org/10.1002/ep.10382.
[39] A.K. Varma, P. Mondal, Pyrolysis of sugarcane bagasse in semi batch reactor: effects of process parameters on product yields and characterization of products, Ind. Crop. Prod. 95 (2017) 704–717, https://doi.org/10.4028/www.scientific.net/MSF.1008.159.
[40] M.A.F. Mazlan, Y. Uemura, N.B. Osman, S. Yusup, Fast pyrolysis of hardwood residues using a fixed bed drop-type pyrolyzer, Energy Convers. Manag. 98 (2015) 208–214, https://doi.org/10.1016/j.enconman.2015.03.102.
[41] M. Asadullah, N.S.A. Rasid, S.A.S.A. Kadir, A. Azdarpour, Production and detailed characterization of bio-oil from fast pyrolysis of palm kernel shell, Biomass Bioenergy 59 (2013) 316–324, https://doi.org/10.1016/j.egypro.2014.12.288.
[42] J.Y. Park, J.-K. Kim, C.-H. Oh, J.-W. Park, E.E. Kwon, Production of bio-oil from fast pyrolysis of biomass using a pilot-scale circulating fluidized bed reactor and its characterization, J. Environ. Manag. 234 (2019) 138–144, https://doi.org/10.1016/j.jenvman.2018.12.104.
[43] K. Rueangsan, P. Kraisoda, A. Heman, H. Tasarod, M. Wangkulangkool, S. Trisupakitti, J. Morris, Bio-oil and char obtained from cassava rhizomes with soil conditioners by fast pyrolysis, Heliyon 7 (2021) e08291, https://doi.org/10.1016/j.heliyon.2021.e08291.